JCTC Journal of Chemical Theory and Computation

Article

pubs.acs.org/JCTC

Counterion Effects on the Denaturing Activity of Guanidinium Cation to Protein

Qiang Shao,[†,‡] Yubo Fan,[§] Lijiang Yang,[†] and Yi Qin Gao*[,†]

[†]Institute of Theoretical and Computational Chemistry, College of Chemistry and Molecular Engineering, Beijing National Laboratory of Molecular Sciences, Peking University, Beijing 100871, China

[‡]Drug Discovery and Design Center, Shanghai Institute of Materia Medica, Chinese Academy of Sciences, 555 Zuchongzhi Road, Shanghai, 201203, China

[§]Bioinformatics and Bioengineering Program, The Methodist Hospital Research Institute, Weill Cornell Medical College, Houston, Texas 77030, United States

Supporting Information

ABSTRACT: The denaturation of a three-α-helix bundle, the B domain of protein A, by guanidinium is studied by molecular dynamics simulations. The simulation results showed that in GdmCl solution, guanidinium cations accumulate around the protein surface, whereas chloride anions are expelled from the protein. In contrast, in GdmSCN solution, both cations and anions accumulate around the protein surface and the degree of Gdm^+ accumulation is higher than that in GdmCl, suggesting the cooperativity between the cations and anions in preferential binding. Moreover, the accumulation of guanidinium around the protein surface is not uniform, and it prefers to populate near residues with negatively charged or planar side chains. On the other hand, guanidinium participates in direct hydrogen bonding with backbone carbonyl groups. Meanwhile, guanidinium also promotes the hydrogen bonding of water to a backbone carbonyl group by changing the hydrogen bonding network within solvent. Therefore, the attack from both water and guanidinium breaks backbone hydrogen bonds and results in the destruction of secondary structures of the protein. The stronger accumulation of guanidinium and more hydrogen bonding from guanidinium in GdmSCN leads to the increase of its denaturing efficiency compared to GdmCl. In the latter solution, the ion pairing between Cl^- and guanidinium limits the approach of guanidinium to protein and the hydrogen bonding between guanidinium and protein, and the main denaturing contributor is the hydrogen bonding from water.

INTRODUCTION

As a protein denaturant, guanidinium chloride (GdmCl) is generally found to be 2 to 2.5 times more effective than another popular denaturant, urea.[1] As a result, it is widely used in various experiments to investigate the folding/unfolding mechanism of proteins.[2−14] For instance, it is used frequently in Φ-value analysis experiments to measure the transition state ensembles (TSE) of protein, which is important in understanding protein folding/unfolding pathways.[15] In single-molecule fluorescence resonance energy transfer (FRET) or NMR experiments, it can be used to study the structure and dynamics of unfolded and intermediate states of proteins and helps illustrate the roles of these states in determining the kinetics and mechanism of protein folding.[16−20] Moreover, it is also used with circular dichroism (CD) spectroscopy to measure the kinetics and thermodynamics of folding transition of proteins.[21]

Because of its extensive use, it is of essential importance to understand the mechanism underlying GdmCl denaturation of the native structures of proteins. Using the combined neutron diffraction with isotopic substitution (NDIS) experiment and molecular dynamics (MD) simulation, Brady and co-workers studied the structure of aqueous GdmCl solution and found that guanidinium cations (Gdm^+) are stacked with each other along their planar water-deficient surfaces, and meanwhile, they form hydrogen bonds with water.[22] Based on this structural characteristic of guanidinium cations in aqueous solution, the authors suggested that GdmCl destabilizes the protein native structure by two kinds of direct interactions between Gdm^+ and protein: (1) Gdm^+ cations accumulate around protein surface and associate with the planar side chains of hydrophobic residues such as tryptophan, tyrosine, and phenylalanine, and (2) Gdm^+ cations form hydrogen bonds with the polar backbone.

The accumulation of Gdm^+ cations around protein surface was observed in many experiments and simulations,[23−26] although a more recent dielectric relaxation spectroscopy (DRS) experiment by Hunger et al. indicated no accumulation of Gdm^+ in both GdmCl and Gdm_2CO_3 solutions.[27] By calculating Gdm^+ cation density around a model peptide, melittin, by MD simulation, Dempsey and co-workers studied the binding of Gdm^+ cations to side chains of protein.[25] It was observed in this simulation that Gdm^+ prefers to stack strongly against the planar side chains of Arg, Trp, and Gln residues but only weakly binds to the hydrophobic groups of peptide, consistent with the speculation of Brady and co-workers.[22] In addition, a recent MD simulation on an amphipathic helical peptide, magainin2, in low-concentration GdmCl solution also indicated the stacking of Gdm^+ ions around the planar charged and/or aromatic side chains of protein.[26]

Received: March 19, 2012
Published: August 22, 2012

dx.doi.org/10.1021/ct3002267 | J. Chem. Theory Comput. 2012, 8, 4364−4373

On the other hand, the direct hydrogen bonding between Gdm^+ and protein backbone and its effects on protein is, however, still a matter of debate. The suggestion that the direct Gdm^+−protein hydrogen bonding is the dominant factor for protein denaturation in the above-mentioned NDIS experiment[22] was supported by several MD simulations.[28,29] However, by measuring acid- and base-catalyzed hydrogen exchange (HX) of a small model peptide using 1D NMR, Englander and co-workers observed that the presence of Gdm^+ cations exerts little effect on either acid- or base-catalyzed HX in GdmCl solution, which hints that Gdm^+ hydrogen bonding with either the NH or the CO group on the backbone of peptide is not significant.[30]

Besides the above-mentioned controversy on the role of direct hydrogen bonding between Gdm^+ and protein backbone in protein denautration, there is another question unanswered: could the presence of Gdm^+ cations alter the water structure, which in turn destabilizes the protein structure in an indirect manner? To answer this question, Mountain and Thirumalai performed MD simulations on GdmCl solution and showed that the local hydrogen-bonding network of water is not altered by Gdm^+ cations.[31] Moreover, by measuring the impact of several protein denaturants (urea and guanidinium ion) and protectants (sugar and trimethylamine N-oxide) on water structure using pressure perturbation calorimetry, Pielak and co-workers observed that there is no correlation between the effect of each cosolvent (denaturant or protectant) on protein structure and its impact on water structure.[32] These results all showed the lack of the importance of the indirect mechanism. On the contrary, the more recent Fourier transform infrared (FTIR) spectroscopy by Vanderkooi and co-workers showed that Gdm^+ cations make hydrogen bonds within the hydrogen bonding network of water more linear.[33] The authors thus suggested the possible existence of indirect mechanism: The solution structure reordering induced by Gdm^+ cations could reduce the entropic penalty for the solvation of hydrophobic residues and therefore impair the hydrophobic packing of protein and lead to protein denaturation.[33]

The effects of Gdm^+ cation on protein structure could be influenced by couterions. For instance, following the Hofmeister series, GdmSCN and GdmCl are strong denaturants whereas Gdm_2SO_4 is a mild protectant. By measuring the hydration structures of Gdm^+ and SCN^- ions in GdmCl and NaSCN solutions, respectively, in the neutron diffraction experiment, Cruickshank and co-workers observed that both ions are weakly hydrated in aqueous solutions,[34] in contrast to the strong hydration of SO_4^{2-} ions suggested by Leberman and Soper.[35] Moreover, using combined neutron diffraction experiment and MD simulations, Brady and co-workers observed strong ion−ion aggregation in Gdm_2SO_4 but not in GdmSCN solution.[36] It was then suggested that in the former solution the strong ion pairing among Gdm^+ and SO_4^{2-} largely reduces the accessibility of Gdm^+ to protein whereas in the latter solution the more randomly distributed ions make Gdm^+ free to bind protein surface. A more recent CD spectroscopy experiment further indicated that the ion paring among Gdm^+ and SO_4^{2-} destroys the ability of Gdm^+ stacking around planar hydrophobic side chains of protein or attenuates its ability of hydrogen bonding to protein backbone.[37] As a result, the β-structured trpzip peptides stabilized by four tryptophans were found to be denatured in GdmCl, but the β-structures were not affected in Gdm_2SO_4 solution. On the other hand, the alanine-based helical peptides, which are relatively unstable in the absence of strong intraprotein hydrophobic interactions by tryptophans, were denatured in both GdmCl and Gdm_2SO_4 solutions because of the hydrogen bonding of guanidinium, although the hydrogen bonding ability of guanidinium becomes weaker in the latter solution.

As shown, MD simulations have been often used to study the protein denaturation in guanidinium solution (normally GdmCl solution). However, the simulations are limited to small peptides. In the present study, we ran MD simulation on the B domain of protein A from *Staphylococcus aureus* (BdpA) in both 4 M GdmCl and 4 M GdmSCN solutions. BdpA consists of 46 residues and adopts a α-helical bundle containing three helices in water:[38] Helix1 (Gln10-His19), Helix2 (Glu25-Asp37), and Helix3 (Ser42-Ala55, as shown in Figure 3a). Of these three helices, Helix2 and Helix3 contact intimately with each other, whereas Helix1 is tilted with an angle of ~30° with respect to the other two helices. As a result, three subdomains are formed (Helix 1−Helix 2 (H1−H2), Helix 2−Helix 3 (H2−H3), and Helix 1−Helix 3 (H1−H3)) by the hydrophobic side chain-side chain interactions among the three helices. The native hydrophobic contacts are listed in Table 1.

Table 1. Summary of Native Hydrophobic Contacts of BdpA

H1−H2 subdomain	H1−H3 subdomain	H2−H3 subdomain
A13−I17	A13−L46	L23−L52
F14−L18	I17−L46	F31−L45
F14−I32	I17−A49	F31−A49
F14−L35	L20−A49	F31−L52
I17−F31	L20−L52	I32−L35
I17−I32		I32−L45
I17−L35		L35−L45
L18−I32		
L20−L23		
L20−F31		

Through the comparative studies on the protein denaturation in two guanidinium solutions, the present study revealed the effects of counterions on the denaturing efficiency of guanidinium as well as the effects on water−protein interaction, which provides molecular insight to the mechanism of guanidinium denaturing protein structure. It was found that, after around 200 ns simulation time, the three helices of BdpA are partially denatured in GdmCl and totally denatured in GdmSCN solutions, consistent with the speculated stronger protein denaturing ability of the latter solution. The detailed analyses of the interactions among guanidinium, water, and protein in both GdmCl and GdmSCN solutions demonstrated that in GdmSCN, the hydrogen bonding from both water and Gdm^+ works as the driving force for protein denaturation. In contrast, in GdmCl, the ion pairing between Gdm^+ and Cl^- limits the approach of Gdm^+ to protein surface and the direct hydrogen bonding from Gdm^+ to protein backbone. As a result, the direct hydrogen bonding between Gdm^+ and protein backbone is weaker in GdmCl and does not contribute to the protein denaturation. Therefore, different counterions have different strengths of ion−ion interactions with guanidinium and thus affect differently the direct interactions of guanidinium to protein. These observations reconcile the differences observed on Gdm^+ hydrogen binding in different studies.[22,28,30]

MATERIALS AND METHODS

All MD simulations were performed at room temperature in explicit solvent making use of the AMBER 9.0 suite of programs[39] with FF99 force field.[40] Water is described with the SPC/E model.[41] Force field parameters for Gdm^+ cation were developed by Jorgensen et al.[42] For BdpA in either GdmSCN or GdmCl solution, three independent trajectories were run. In each simulation system, the initial structure of BdpA was taken from its NMR structure (PDB code: 1BDD), which was placed into a cubic box containing 665 guanidinium, equal amount of anions (SCN^- or Cl^-), and a large number of water molecules (5057 water in GdmSCN and 5064 water in GdmCl solution). The concentration of guanidinium was thus controlled to be ~4 M for the two solutions. Three Na^+ cations were then added into the box to neutralize the charge of the system. Meanwhile, BdpA in pure water (4346 water) was also studied, and the simulation result was compared to those in solutions containing guanidinium. Moreover, to see the effects of force fields of Gdm^+ and water on simulation results, four additional simulations using the various combinations of Gdm^+ (Jorgensen et al.[42] and MacKerell et al.[43]) and water (SPC/E model[41] and TIP3P[44]) force fields were also run. The details of simulations are listed in Table 2.

Table 2. Parameters for Individual Simulations

solution		Gdm^+ force field	water force field	simulation length (ns)
GdmSCN	Traj 1	Jorgensen et al.	SPC/E	220
	Traj 2			180
	Traj 3			190
GdmCl	Traj 1	Jorgensen et al.	SPC/E	190
	Traj 2			180
	Traj 3			190
water	Traj 1	Jorgensen et al.	SPC/E	190
GdmSCN	Traj 1	Jorgensen et al.	TIP3P	110
	Traj 1	MacKerell et al.	SPC/E	110
GdmCl	Traj 1	Jorgensen et al.	TIP3P	120
	Traj 1	MacKerell et al.	SPC/E	120

For each system, the simulation procedure included the energy minimization, the following heating-up process, and the final longtime equilibrium simulation calculation (production). *NPT* (number, pressure, temperature) ensemble calculations were performed and periodic boundary conditions were used in the simulations. The SHAKE algorithm[45] was used to constrain all bonds involving hydrogen atoms. A cutoff of 10.0 Å was applied for nonbonding interactions. The Particle Mesh Ewald method was applied to treat long-range electrostatic interactions.[46]

The energy of each system was minimized through a total of 2500 steps of calculations: 1000 steps of steepest descent minimization with the peptide being fixed using harmonic restraints (using a force constant of 500.0 kcal mol^{-1} $Å^{-2}$ to apply to the backbone atoms), which was then followed by 1500 steps of conjugate gradient minimization. Subsequently, to better relax the system, the system was heated to 360 K and equilibrated for several nanoseconds at 360 K, followed by a 200 ps of cooling from 360 to 300 K performed with harmonic restraints (force constant = 10.0 kcal mol^{-1} $Å^{-2}$) applied to the backbone atoms. The three independent trajectories of each solution system were different in the running time used to equilibrate the system at 360 K. Finally, production runs around 200 ns were performed at 300 K and then used for the data analysis, with the data being collected every 1.0 ps.

Hydrogen Bond Definition. A hydrogen bond is considered as formed only if the distance between the two heavy atoms of the hydrogen donor and acceptor is less than 3.2 Å and the N−H−O (or O−H−O) angle is greater than 135°.

RESULTS

Effects of Guanidinium Solutions on the Structure of BdpA. After ~200 ns simualtions, three independent trajectories for BdpA in each guanidinium solution reached similar (solution-dependent) stable conformations. To examine the secondary structures and hydrophobic clustering of BdpA, we show in Figure 1 a typical trajectory of the root-mean-square deviation (rmsd) of BdpA with respect to its NMR structure, and the radius of gyration (R_g) in GdmSCN, GdmCl, and pure water as a function of simulation time. The data from the other two trajectories for BdpA in both GdmSCN and GdmCl solutions are given in Figures S1 and S2 in the Supporting Information.

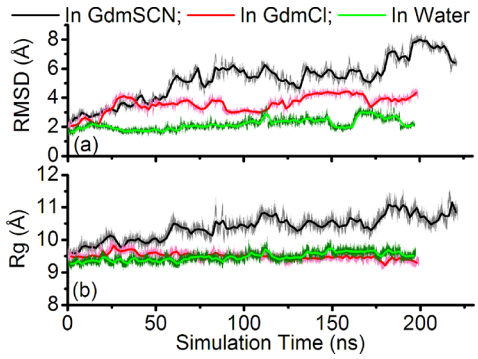

Figure 1. (a) rmsd; (b) R_g of the B domain of protein A (BdpA) as a function of simulation time in three different solutions: black, GdmSCN; red, GdmCl; green, pure water. Data were collected from one typical trajectory for each solution.

As shown in Figure 1, the rmsd value of BdpA in GdmSCN was apparently greater than that in pure water, while the rmsd value in GdmCl was in between. Meanwhile, the R_g value was increased in GdmSCN but not changed significantly in GdmCl solution compared to that in pure water. Similar changing tendencies of rmsd and R_g in the two guanidinium solutions can be also seen in the other two sets of independent trajectories (Figures S1−S2 in the Supporting Information). To further understand the structure change of BdpA in the three solutions, we next calculated the number of native hydrophobic contacts formed within BdpA in the corresponding solutions as a function of simulation time. The native hydrophobic contacts were given in Table 1. The side chains of two hydrophobic residues are considered as in contact only if the distance between side chains is within 5 Å. During the simulation, the number of native hydrophobic contacts dropped quickly in GdmSCN solution whereas in the other two solutions this number only slightly fluctuated (Figure 2a). The breaking of the hydrophobic contacts in GdmSCN solution, as shown in Figure 2b, was mainly seen for those in the H1−H3 subdomain. As a result, in the final structure of BdpA in GdmSCN solution (Figure 3), the N-terminus of BdpA (Helix1, green color) moved away from the C-terminus (Helix3, purple color) and

dx.doi.org/10.1021/ct3002267 | J. Chem. Theory Comput. 2012, 8, 4364−4373

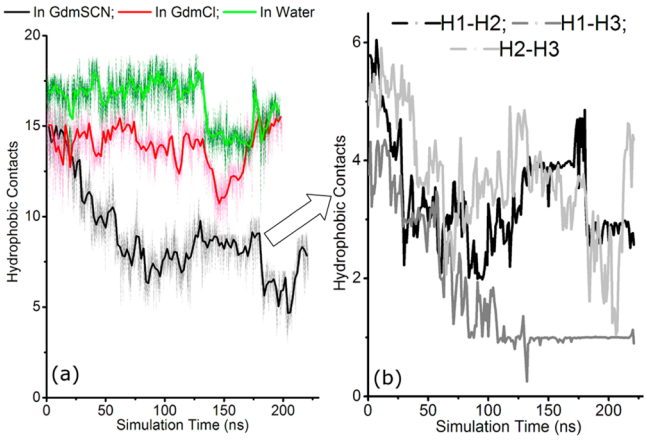

Figure 2. (a) Number of native hydrophobic side chain-side chain contacts formed in the entire protein of BdpA as a function of simulation time in GdmSCN, GdmCl, and water solutions. (b) Number of contacts formed in the three subdomain (H1−H2, H1−H3, and H2−H3) of BdpA as a function of simulation time in GdmSCN solution.

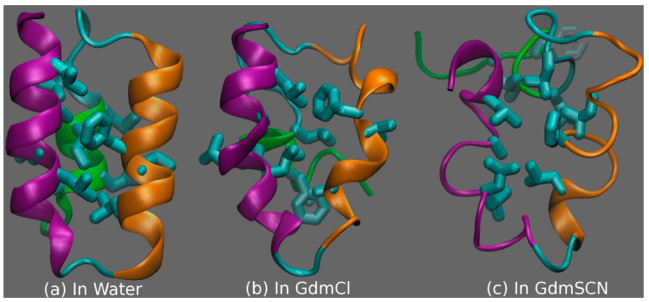

Figure 3. Simulated structures of BdpA in GdmSCN and GdmCl solutions and the comparison to the corresponding stable structure in pure water. Side chains forming the hydrophobic core cluster in the center of BdpA are shown with licorice mode, and the three helices are shown in different colors: Helix1, green; Helix2, orange; Helix3, purple.

few side chain contacts between the two helices exist. In contrast, in GdmCl and water, the N- and C-terminal helices remain in contact. The end-to-end distance of the protein in each solution was then calculated and the distribution was shown in Figure S3 in the Supporting Information. It is clear to see that the distribution of end-to-end distance was much broader in GdmSCN than in other two solutions, indicating the higher flexibility of protein structure in the presence of GdmSCN.

To see the effects of the two guanidinium solutions on the secondary structures of BdpA in details, we demonstrated in Figure 4 the survival probability of individual backbone hydrogen bonds in the two solutions. There are totally 25 backbone hydrogen bonds in the native structure of BdpA, and these hydrogen bonds are numbered from N- to C- terminus (HBs 1−5 in Helix1, HBs 6−15 in Helix2, and HBs 16−25 in Helix3, see Table 3). One can see from Figure 4 that after ∼200 ns simulation, on average, less than one hydrogen bond remained in each helix in GdmSCN solution. By contrast, several hydrogen bonds remained intact in GdmCl solution (3 HBs in Helix2 and 6 HBs in Helix3). Therefore, combining the results shown in Figures 1−4, it is clearly seen that the guanidinium-induced denaturation of BdpA was more severe in GdmSCN than in GdmCl solution.

Table 3. Summary of Backbone Hydrogen Bonds within the Three Helices of BdpA

Helix1		Helix2		Helix3	
HB1	Q10O−F14H	HB6	E25O−N29H	HB16	Q41O−L45H
HB2	Q11O−Y15H	HB7	E26O−G30H	HB17	S42O−L46H
HB3	N12O−E16H	HB8	Q27O−F31H	HB18	A43O−A47H
HB4	A13O−I17H	HB9	R28O−I32H	HB19	N44O−E48H
HB5	F14O−L18H	HB10	N29O−Q33H	HB20	L45O−A49H
		HB11	G30O−S34H	HB21	L46O−K50H
		HB12	F31O−L35H	HB22	A47O−K51H
		HB13	I32O−K36H	HB23	E48O−LS2H
		HB14	Q33O−D37H	HB24	A49O−N53H
		HB15	S34O−D38H	HB25	K50O−D54H

On the other hand, the stability of three helices of BdpA in the two solutions followed the order of Helix3 > Helix2 > Helix1, consistent with the observations of several previous experiments. For example, it was observed that the isolated Helix3 fragment folds into the helical structure in the aqueous solution with the helix population of ∼30% whereas the other two fragments of Helix1 and Helix2 have no detectable helical content.[47] In addition, the earlier fluorescence experiment by

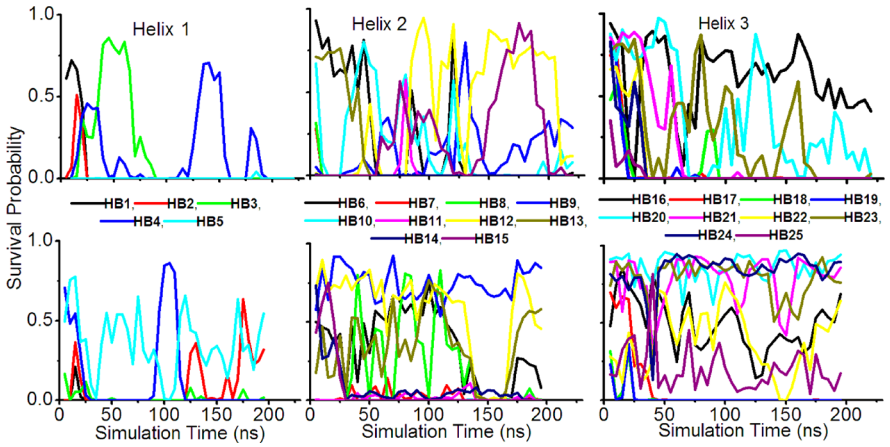

Figure 4. Breaking and formation of individual backbone hydrogen bonds in three helices of BdpA in GdmSCN (top panel) and GdmCl (bottom panel), respectively.

dx.doi.org/10.1021/ct3002267 | J. Chem. Theory Comput. 2012, 8, 4364−4373

Bottomley et al. showed that during the GdmCl-induced denaturation of Trp-substituted BdpA Helix1 unfolds first, followed by Helix2 and Helix3.[48] Using T-jump fluorescence measurement on Tyr15 residue in Helix1, Vu et al. indicated that in the intermediate state of BdpA both Helix2 and Helix3 are formed while Helix1 is not.[49] We also observed in our previous folding simulation of BdpA using integrated tempering sampling molecular dynamics simulation method[50] that, along the lowest free energy folding pathway of BdpA, the formation and stability of the three helices follows the same order.[51]

Accumulation of Guanidinium around Protein Surface of BdpA. To understand the mechanism of guanidinium-induced denaturation of BdpA, we studied the molecular interactions between guanidinium and protein. We first calculated the number of various ions and water molecules in the proximity to the protein surface (6 Å) after BdpA reached its stable structures in GdmSCN and GdmCl solutions. The number distribution was shown in Figure 5, and the average

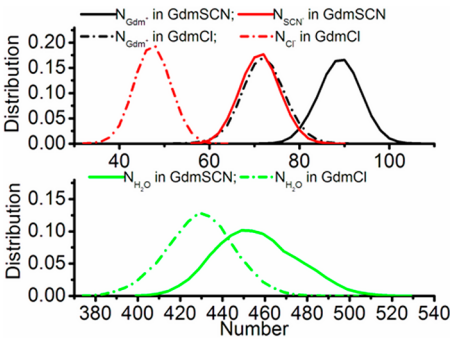

Figure 5. Distribution of the number of Gdm^+ cations, SCN^- (Cl^-) anions, and water molecules within 6 Å of protein surface in GdmSCN (GdmCl) solutions.

number was 90.0 for Gdm^+ cation, 72.2 for SCN^- anion, and 445.5 for water in GdmSCN solution, and 73.0 for Gdm^+ cation, 48.4 for Cl^- anion, and 431.8 for water in GdmCl solution. Using the ratio between the numbers of Gdm^+ and water molecules within 6 Å of the protein surface, normalized according to the total numbers of Gdm^+ and water molecules in the simulation system,

$$R_{gdm} = \frac{(n_{gdm}/n_{water})_{surface}}{(n_{gdm}/n_{water})_{total}} \quad (1)$$

we can easily see that Gdm^+ cations always accumulated on the protein surface in the solutions (R_{gdm} is 1.53 and 1.28 in GdmSCN and GdmCl solutions, respectively). More importantly, the accumulation of Gdm^+ cations was stronger in the presence of SCN^- than when Cl^- anions are present. Accordingly, SCN^- also accumulated around the protein surface (R_{SCN} = 1.28) in GdmSCN solution, although it did not accumulate as much as Gdm^+ cations. By contrast, instead of clustering around the protein surface, Cl^- anions preferred to stay in the bulk solution and were expelled from the protein surface (R_{Cl} = 0.85).

To obtain more details of guanidinium clustering around the protein surface, we next calculated the average number of Gdm^+ cations and the counteranions as well as water within 6 Å of individual residues. The results were given in Tables 4 and 5, for GdmSCN and GdmCl solutions, respectively. The residues, which had close contacts with guanidinium, as revealed by the large number of surrounded Gdm^+ cations but simultaneous small number of anions, were mainly negatively charged residues (e.g., Glu16, Glu25, Glu26, Asp37, Asp38, Glu48, and Asp54) and the residues with planar side chains (e.g., Phe14, Tyr15, Asn22, Gln27, Asn44, and Asn53), along with some polar ones (e.g., Q27 and S40).

Figure 6 showed the radial distribution functions (RDF) of different atoms of guanidinium and water around backbone carbonyl groups (C═O) and side chains of several representative residues from BdpA with either charged (E26, K36), hydrophobic (I32), or planar (N44) side chains. The data were collected from the simulation of BdpA in GdmSCN solution. It is clearly seen that, for all these residues, there are high peaks in the RDF diagram for the backbone carbonyl groups, demonstrating the formation of hydrogen bonds between guanidinium and carbonyl groups. Moreover, for negatively charged E26 residue, there is also a high peak in the RDF around its side chain, showing the association between guanidinium and the side chain. Meanwhile, guanidinium also preferentially binds the side chain of N44. The analysis of the snapshots from the simulation indicated that guanidinium ions stacked with the planar side chain of N44 in the same manner as described in the previous studies.[25,26] On the contrary, guanidinium was expelled from the positively charged and hydrophobic side chains of K36 and I32, respectively.

Hydrogen Bonding Interactions of Guanidinium and Water with BdpA. Figure 7 shows the total number of hydrogen bonds formed between the residues (including both −CO and −NH groups), which are involved in the formation of backbone hydrogen bonds in the three helices of BdpA, and water or guanidinium as a function of simulation time in GdmSCN and GdmCl solutions. One can see from this figure that the breaking of backbone hydrogen bonds correlated well with the increase of hydrogen bonds formed between the backbone carbonyl groups and water or guanidinium (both as hydrogen bonding donors). This correlation was more apparent in GdmSCN than in GdmCl solution (Figure 7a). On the other hand, the number of hydrogen bonds formed between the backbone amide groups and water (as hydrogen bonding acceptor) is small and does not correlate with the breaking of backbone hydrogen bonds.

To investigate the role of water and guanidinium participating in inducing the breaking of backbone hydrogen bonds of BdpA in GdmSCN, the hydrogen bond formation between solvent/cosolvent and carbonyl groups of individual residues were also analyzed (considering the rather large number of backbone hydrogen bonds within BdpA, nine residues were selected for the analysis, with three residues chosen from each helix). One can see from Figure 8 that the breaking of each backbone hydrogen bond is accompanied by the formation of hydrogen bonds between the corresponding carbonyl group and water/guanidinium. Therefore, these results (Figures 7 and 8) suggested that the breaking of backbone hydrogen bonds is likely initiated by the attack of the protein carbonyl group by both water and guanidinium.

Interactions between Solvents. Besides the interactions with protein as indicated (hydrogen bonding to backbone carbonyl groups and packing to side chains), guanidinium cations also interact with anions (ion−ion interactions) and water (hydrogen bonding interactions). Figure 9 showed the RDF of guanidinium around anions (SCN^- or Cl^-) and water in GdmSCN and GdmCl solutions, respectively. One can see from Figure 9a that the peak at

dx.doi.org/10.1021/ct3002267 | J. Chem. Theory Comput. 2012, 8, 4364−4373

Table 4. Average Number of Cosolvent (Gdm^+ and SCN^- Ions) and Solvent (Water) Molecules within 6 Å of Each Individual Residue of BdpA in GdmSCN Solution[a]

in GdmSCN									
residue no.	N_{H2O}	N_{Gdm+}	N_{SCN-}	$N_{Gdm+} - N_{SCN-}$	residue no.	N_{H2O}	N_{Gdm+}	N_{SCN-}	$N_{Gdm+} - N_{SCN-}$
Q10	43.93	9.20	7.93	1.27	Q33	32.64	7.87	6.03	1.84
Q11	42.35	8.91	7.80	1.11	S34	19.43	6.06	3.71	2.35
N12	33.60	7.66	6.14	1.52	L35	13.27	4.62	2.22	2.40
A13	22.32	6.01	4.54	1.47	K36	37.79	9.19	6.25	2.94
F14	43.41	8.77	6.58	2.19	D37	25.48	6.87	4.75	2.12
Y15	34.35	7.91	5.68	2.23	D38	19.98	6.56	3.21	3.35
E16	18.09	6.37	4.30	2.07	P39	33.13	8.66	5.17	3.49
I17	18.88	5.36	4.45	0.91	S40	25.75	6.81	4.07	2.74
L18	27.01	5.84	4.68	1.16	Q41	23.38	6.52	4.29	2.23
H19	23.52	6.16	3.87	2.29	S42	16.66	5.29	2.92	2.37
L20	8.66	3.46	1.93	1.53	A43	25.97	6.32	3.91	2.41
P21	20.87	6.16	3.74	2.42	N44	30.10	7.67	4.78	2.89
N22	26.77	7.60	4.53	3.07	L45	21.32	6.68	3.48	3.20
L23	22.23	5.51	3.84	1.67	L46	23.09	5.88	4.84	1.04
N24	28.34	7.63	4.61	3.02	A47	24.36	5.85	4.51	1.34
E25	30.82	8.21	5.33	2.88	E48	26.61	7.42	4.69	2.73
E26	33.28	8.69	5.96	2.73	A49	10.69	3.73	2.60	1.13
Q27	34.26	7.83	5.83	2.00	K50	36.28	9.12	7.73	1.39
R28	25.34	6.84	4.89	1.95	K51	33.57	9.59	6.93	2.66
N29	25.94	6.43	4.67	1.76	L52	15.05	5.83	2.43	3.40
G30	14.77	4.36	3.19	1.17	N53	16.67	7.47	3.15	4.32
F31	21.36	5.42	4.11	1.31	D54	27.70	9.20	4.91	4.29
I32	18.17	4.72	3.59	1.13	A55	26.57	7.96	4.35	3.61

[a]The average is over the last 50 ns of the simulation. The fifth column is the number difference of Gdm^+ and SCN^- ions.

Table 5. Average Number of Cosolvent (Gdm^+ and Cl^- ions) and Solvent (Water) Molecules within 6 Å of Each Individual Residue of BdpA in GdmCl Solution[a]

in GdmCl									
residue no.	N_{H2O}	N_{Gdm+}	N_{Cl-}	$N_{Gdm+} - N_{Cl-}$	residue no.	N_{H2O}	N_{Gdm+}	N_{Cl-}	$N_{Gdm+} - N_{Cl-}$
Q10	43.99	7.07	5.18	1.89	Q33	35.11	5.90	3.60	2.30
Q11	35.64	5.26	3.91	1.35	S34	21.16	4.25	1.66	2.59
N12	34.99	5.79	3.74	2.05	L35	14.20	2.66	0.48	2.18
A13	17.84	3.08	1.39	1.69	K36	35.54	6.05	3.38	2.67
F14	20.16	3.25	1.32	1.93	D37	28.81	6.83	2.31	4.52
Y15	36.89	6.98	3.47	3.51	D38	25.03	6.88	1.66	5.22
E16	27.92	5.46	2.61	2.85	P39	26.93	5.93	2.28	3.65
I17	10.04	1.68	0.26	1.42	S40	30.68	6.72	2.88	3.84
L18	24.74	4.50	2.13	2.37	Q41	39.85	8.50	3.89	4.61
H19	35.70	6.50	3.47	3.03	S42	18.33	3.91	1.26	2.65
L20	22.73	3.95	1.76	2.19	A43	22.23	4.03	1.85	2.18
P21	37.38	6.56	3.61	2.95	N44	31.37	5.85	2.92	2.93
N22	27.37	6.96	2.16	4.80	L45	23.69	4.32	1.82	2.50
L23	13.35	3.10	1.07	2.03	L46	17.77	3.25	1.20	2.05
N24	29.25	6.55	2.88	3.67	A47	21.74	3.41	1.95	1.46
E25	32.61	6.89	3.06	3.83	E48	25.62	4.69	1.80	2.89
E26	35.67	7.45	2.96	4.49	A49	5.01	0.73	0.00	0.73
Q27	29.01	5.99	2.61	3.38	K50	31.95	6.01	3.01	3.00
R28	20.74	3.60	1.47	2.13	K51	40.20	8.23	3.93	4.30
N29	28.43	4.80	2.44	2.36	L52	26.51	6.04	1.98	4.06
G30	20.54	3.21	1.60	1.61	N53	19.85	5.75	1.31	4.44
F31	19.57	3.26	1.16	2.10	D54	28.73	8.39	2.45	5.94
I32	15.18	2.23	1.11	1.12	A55	29.92	8.40	2.49	5.91

[a]The average is over the last 50 ns of the simulation. The fifth column is the number difference of Gdm^+ and Cl^- ions.

around ~2 Å, referring to the distance between the hydrogen atom of guanidinium and anion, is much lower in GdmSCN than in GdmCl, indicating the weaker ion−ion interactions between Gdm^+ and SCN^- than that between Gdm^+ and Cl^-. Meanwhile, the peak of RDF of Gdm^+ around water is higher in GdmSCN than in GdmCl (Figure 9b), which indicates that

dx.doi.org/10.1021/ct3002267 | J. Chem. Theory Comput. 2012, 8, 4364−4373

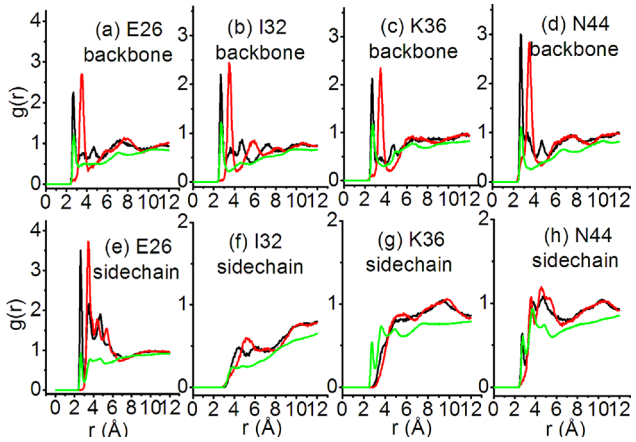

Figure 6. Radial distribution functions ($g(r)$) for different atoms of Gdm^+ and water around the backbone CO groups and side chains of four residues (E26, I32, K36, and N44) at the last 50 ns of the simulation of BdpA in GdmSCN solution (Black line: Gdm^+ nitrogen atoms around residue backbone CO groups or side chains. Red line: Gdm^+ carbon atoms around residue backbone CO groups or side chains. Green line: water oxygen atoms around residue backbone CO groups or side chains).

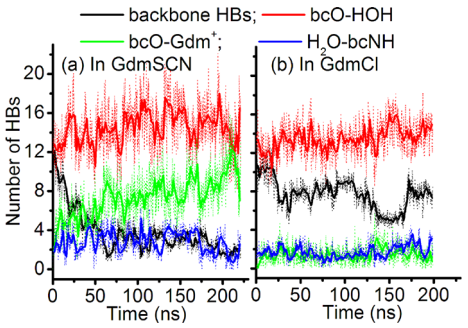

Figure 7. Breaking and formation of hydrogen bonds for residues involved in all backbone hydrogen bonds of BdpA in (a) GdmSCN and (b) GdmCl solutions (Back line: the number of backbone hydrogen bonds. Red line: the number of hydrogen bonds formed between carbonyl groups and water as hydrogen bonding donor. Green line: the number of hydrogen bonds formed between carbonyl groups and Gdm^+ as hydrogen bonding donor. Blue line: the number of hydrogen bonds formed between amide groups and water as hydrogen bonding acceptor).

Gdm^+ has relatively stronger hydrogen bonding with water in the former solution.

To see more clearly the effects of hydrogen bonding between Gdm^+ and water on the properties of water, we next calculated the hydrogen bond number formed per water in GdmSCN and GdmCl solutions, and the results were compared to that in pure water (Figure 10). The hydrogen bond number formed per water to Gdm^+ is 0.96 in GdmSCN, 0.90 in GdmCl. Meanwhile, the number of hydrogen bonds formed to other water molecules per water molecule is 1.95 in GdmSCN, 2.00 in GdmCl, and 3.06 in pure water. Therefore, the total number of hydrogen bond formed per water is slightly larger in pure water than in GdmSCN and GdmCl solutions.

Furthermore, the hydrogen bonding among solvent (water and guanidinium) can be separated into two contributions: the hydrogen bonds with water being the hydrogen bonding acceptor ($\underline{H_2O}\cdots HOH$ and $\underline{H_2O}\cdots Gdm^+$) and those with water as hydrogen bonding donor ($\underline{HOH}\cdots OH_2$). As shown in Figure

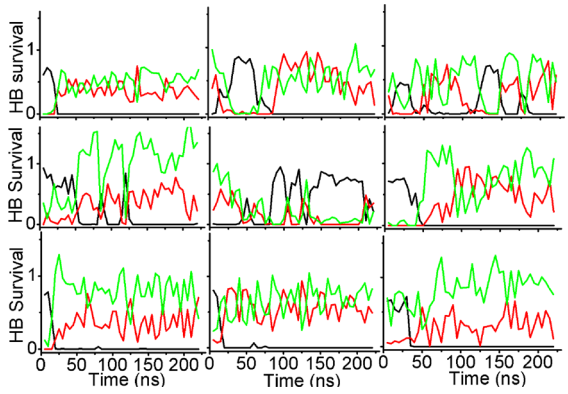

Figure 8. Breaking and formation of hydrogen bonds for individual residues involved in nine backbone hydrogen bonds of BdpA in GdmSCN solution (Back line: the number of backbone hydrogen bonds. Red line: the number of hydrogen bonds formed between carbonyl group and water as hydrogen bonding donor. Green line: the number of hydrogen bonds formed between carbonyl group and Gdm^+ as hydrogen bonding donor).

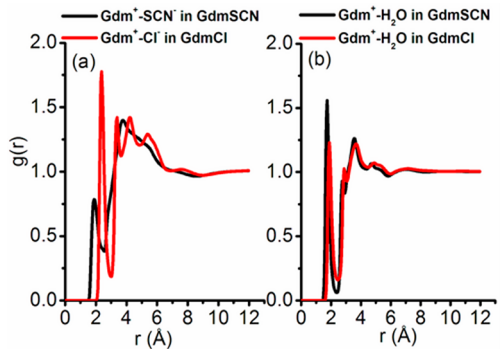

Figure 9. Radial distribution functions for Gdm^+ around (a) counterions (SCN^- or Cl^-) and (b) water at the last 50 ns of the simulations of BdpA in GdmSCN and GdmCl solutions, respectively.

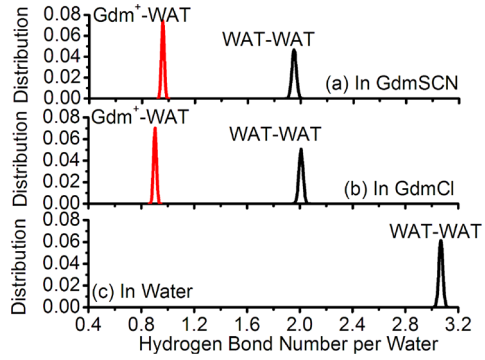

Figure 10. Distribution of the hydrogen bond number formed per water molecule (including hydrogen bonds among water and water, and water and Gdm^+) in three simulation systems: (a) GdmSCN, (b) GdmCl, and (c) pure water.

10, the number of hydrogen bonds per water as an acceptor is 1.94 in GdmSCN, 1.90 in GdmCl, and 1.53 in pure water, and the number of hydrogen bonds per water as a donor is 0.97 in GdmSCN, 1.00 in GdmCl, and 1.53 in pure water, respectively. Therefore, the addition of the denaturants rich in proton donors changed the equilibrium between proton donor and acceptor of water: Compared to pure water, the GdmCl and GdmSCN solutions have a larger number of free water

dx.doi.org/10.1021/ct3002267 | J. Chem. Theory Comput. 2012, 8, 4364−4373

hydrogen donors, which could then form hydrogen bonds with backbone carbonyl groups in protein, thus playing a potentially important role in denaturing protein secondary structures (see Figure 8). In addition, compared to Cl^-, SCN^- has weaker ion−ion interactions with Gdm^+ (Figure 9), and thus, Gdm^+ has more freedom to interact with protein, which explains why GdmSCN is more efficient than GdmCl in denaturing BdpA.

Force Field Influence on Simulation Results. In principle, the accuracy of a molecular dynamics simulation largely depends on the force field used. To test how force field used affects counterion effects on the denaturing activity of guanidinium, in the present study, another set of force field parameters of guanidinium, which were taken from the CHARMM22 force field by MacKerell et al.,[43] was also used in the denaturation simulation. Meanwhile, to see the effects of water model used on the simulation results, TIP3P solvent model[44] was also used besides the SPC/E model, as mentioned previously. The combination of Gdm^+ force fields and solvent models can be seen in Table 2 for each simulation.

The denaturation process of BdpA in either GdmSCN or GdmCl using different force fields (Gdm^+ force field of Jorgensen et al. + TIP3P (SPC/E), MacKerell et al. + TIP3P (SPC/E)), were shown in Figure S4 in the Supporting Information, represented by the time series of the number of backbone hydrogen bonds formed within BdpA. It is clearly seen that the number of backbone hydrogen bonds decreases in all simulation solutions, indicating the denaturation of protein. In addition, the hydrogen bond number decrease is always more apparent in GdmSCN than in GdmCl, no matter what force fields were used. Therefore, consistent with the earlier observation, GdmSCN has the stronger denaturing effects than GdmCl does.

The number distribution of various ions and water molecules in the proximity to the protein surface (6 Å) of BdpA was also calculated for each comparative simulation system and the results were shown in Figure S5 in the Supporting Information. This figure is very similar to Figure 6, and both figures demonstrated the same tendency of Gdm^+: Gdm^+ accumulates on protein surface in both GdmSCN and GdmCl solutions and the accumulation in the former solution is stronger than in the latter solution.

Figures S6 and S7 in the Supporting Information show the total number of hydrogen bonds formed between the backbone carbonyl groups, which are involved in the formation of backbone hydrogen bonds in the three helices of BdpA, and water/guanidinium as a function of simulation time in each comparative simulation system. It is easy to see that the breaking of backbone hydrogen bonds always correlates well with the increase of hydrogen bonds formed between the backbone carbonyl groups and water or guanidinium, which is in agreement with the observation of Figure 7. Therefore, all results (Figures S4−S7 in the Supporting Information) from comparative simulations pointed to the same role of Gdm^+ denaturing protein structure as described in the simulations using Gdm^+ force field of Jorgensen et al. and SCP/E model, indicating the very few influence of force field on the quantitative description of Gdm^+ activity in the present study.

DISCUSSION AND CONCLUSIONS

Denaturing osmolytes have attracted much attention in the last several decades. Various experimental measurements and theoretical approaches have been used to study the molecular interactions between solute and solvent in osmolyte/water mixed solutions, and the preferential direct interactions between protein and denaturing osmolytes were considered in these studies as the dominant driving force for protein unfolding induced by the latter molecules.[52−69] As an efficient denaturing osmolyte, the direct interactions between guanidinium and protein were suggested in many studies to include not only the stacking of guanidinium around the planar side chains but also the formation of hydrogen bonds toward the polar backbone.[22,25,26,28,70] However, the recent hydrogen−deuterium exchange experiment indicated that Gdm^+ does not form hydrogen bonds with peptide in GdmCl solution.[30]

In the present study, we used a 46-residue protein, the B domain of protein A from *Staphylococcus aureus* (BdpA) as the model, and ran MD simulations on BdpA in both GdmSCN and GdmCl solutions. Several force fields of guanidinium cation and water were tested, and similar results were obtained in the corresponding simulations. Through the present study, we attempted to investigate the molecular interactions between protein and water/guanidinium, which gives the detailed information of guanidinium denaturing protein and the counterion effects on the protein denaturing ability of guanidinium.

It was found in the present study that Gdm^+ accumulates around protein surface in both GdmSCN and GdmCl solutions. The degree of guanidinium accumulation is heavier in the former solution than in the latter. SCN^- also shows preferential binding, but Cl^- is expelled from the protein surface in their corresponding solutions. Therefore, both Gdm^+ and SCN^- ions are weakly hydrated, but Cl^- ion is strongly hydrated in aqueous solution. This phenomenon can be explained by the simple concept of ion pairing proposed by Collins, of which small ions having a high surface charge density were suggested to bind water molecule strongly (defined as "kosmotropes") whereas big ions bind water weakly ("chaotropes").[71,72] Guanidinium and thiocyanate have low surface charge density and are thus weakly hydrated. As a result, these two ions bind directly to protein tightly. Chloride anion, which has higher charge density than thiocyanate, has the lower tendency to bind to protein. On the other hand, Collins also proposed that, in addition to the ion pairing between small ions of opposite charge, two big ions can also form ion pairs because of the more favorable medium−medium interactions formed by the released water molecules.[72] Therefore, the relatively expelled chloride anions could form ion pairs with guanidinium cations and therefore limit the latter to approach the protein. As a result, the protein denaturing ability of guanidinium is enhanced as it is coupled with SCN^- ion.

As Gdm^+ ions accumulate around protein, they prefer to be around negatively charged residues and the residues with planar side chains. Meanwhile, Gdm^+ cations, along with water molecules, participate in the direct hydrogen bonding with the backbone carbonyl groups, which leads to the breaking of backbone hydrogen bonds and the consequent secondary structure destruction. Therefore, guanidinium denatures protein by not only direct interacting toward protein (direct stacking around protein side chains, and direct hydrogen bonding toward backbone carbonyl groups) but also promoting the hydrogen bonding between water and backbone carbonyl groups.

It is worth noting that, along with the alleviation of Gdm^+ accumulation on protein surface by replacing SCN^- by Cl^-, the direct hydrogen bonding of Gdm^+ to backbone carbonyl groups is also impaired. It is very clear to see from Figure 7 and Figures

S6 and S7 in the Supporting Information that the correlation between the breaking of backbone hydrogen bonds and the increase of hydrogen bonds formed between the backbone carbonyl groups and guanidinium is always strong in GdmSCN but always very weak in GdmCl solution. Therefore, in the latter solution, the breaking of backbone hydrogen bonds is mainly induced by the hydrogen bonding from water but not guanidinium. This observation is actually consistent with the experimental observation by Englander and co-workers:[30] GdmCl slows either acid- or base-catalyzed HX to only a minor degree, which hints that Gdm^+ hydrogen bonding with either NH or CO group on the backbone of peptide is not significant in GdmCl solution.

The model of Gdm^+ denaturing protein observed here is consistent with the mechanism of urea denaturing protein except that the binding interactions to side chains are nonexistent for urea, which was observed by the recent MD simulation studies by Wei et al.[73−75] Urea prefers to bind to protein surface, making the surrounding water interact with carbonyl groups more actively and thus initiating the breaking of backbone hydrogen bonds; meanwhile, urea also forms hydrogen bonds with carbonyl groups in the denaturation process[76] and, more importantly, forms hydrogen bonds with amide groups in the denatured protein structure and therefore stabilize the denatured state.

■ ASSOCIATED CONTENT

Supporting Information

Data for the second and third independent simulation trajectories for BdpA in GdmSCN and GdmCl solutions; the distribution of end-to-end distance of BdpA in GdmSCN and GdmCl solutions; the trajectories of comparative simulations of BdpA in GdmSCN and GdmCl solutions using different force fields; the distribution of the number of Gdm^+ cations, SCN^- (Cl^-) anions, and water molecules within 6 Å of protein surface in each comparative simulation system; the breaking and formation of hydrogen bonds for residues involved in all backbone hydrogen bonds of BdpA in each comparative simulation system. This material is available free of charge via the Internet at http://pubs.acs.org.

■ AUTHOR INFORMATION

Corresponding Author

*Tel: +86-010-62752431. E-mail: gaoyq@pku.edu.cn.

Notes

The authors declare no competing financial interest.

■ ACKNOWLEDGMENTS

This work was supported by research grants from the National Natural Science Foundation of China (91027044 and 21125311 to Y.Q.G, and 21003003 to Q.S.). Y.Q.G. is a 2008 Changjiang Scholar. For the computations in this article, we used the computation resource in Shanghai Supercomputing Center (SSC), and supercomputing facilities at The Texas Advanced Computing Center (TACC) at The University of Texas at Austin (Project ID: TG-MCB110130) and BlueBioU at Rice University.

■ REFERENCES

(1) Myers, J. K.; Pace, C. N.; Scholtz, J. M. *Protein Sci.* **1995**, *4*, 2138−2148.
(2) Ibarra-Molero, B.; Loladze, V. V.; Makhatadze, G. I.; Sanchez-Ruiz, J. M. *Biochemistry* **1999**, *38*, 8138−8149.
(3) Sasahara, K.; Sakurai, N.; Nitta, K. *J. Mol. Biol.* **1999**, *291*, 693−701.
(4) Pappenberger, G.; Saudan, C.; Becker, M.; Merbach, A. E.; Kiefhaber, T. *Proc. Natl. Acad. Sci. U.S.A.* **2000**, *97*, 17−22.
(5) Akhtar, M. S.; Ahmad, A.; Bhakuni, V. *Biochemistry* **2002**, *41*, 3819−3827.
(6) Liu, W.; Cellmer, T.; Keerl, D.; Prausnitz, J. M.; Blanch, H. W. *Biotechnol. Bioeng.* **2005**, *90*, 482−490.
(7) Dempsey, C. E.; Piggot, T. J.; Mason, P. E. *Biochemistry* **2005**, *44*, 775−781.
(8) Moglich, A.; Krieger, F.; Kiefhaber, T. *J. Mol. Biol.* **2005**, *345*, 153−162.
(9) Dar, T. A.; Singh, L. R.; Islam, A.; Anjum, F.; Moosavi-Movahedi, A. A.; Ahmad, F. *Biophys. Chem.* **2007**, *127*, 140−148.
(10) Chang, H. P.; Chou, C. Y.; Chang, G. G. *Biophy. J.* **2007**, *92*, 1374−1383.
(11) Nettels, D.; Muller-Spath, S.; Kuster, F.; Hofmann, H.; Haenni, D.; Ruegger, S.; Reymond, L.; Hoffmann, A.; Kubelka, J.; Heinz, B.; Gast, K.; Best, R. B.; Schuler, B. *Proc. Natl. Acad. Sci. U.S.A.* **2009**, *106*, 20740−20745.
(12) Chang, J. Y. *Biochemistry* **2009**, *48*, 9340−9346.
(13) Hatfield, M. P. D.; Murphy, R. F.; Lovas, S. *J. Phys. Chem. B* **2011**, *115*, 4971−4981.
(14) Heyda, J.; Kozisek, M.; Bednarova, L.; Thompson, G.; Konvalinka, J.; Vondrasek, J.; Jungwirth, P. *J. Phys. Chem. B* **2011**, *115*, 8910−8924.
(15) Sato, S.; Religa, T. L.; Daggett, V.; Fersht, A. R. *Proc. Natl. Acad. Sci. U.S.A.* **2004**, *101*, 6952−6956.
(16) Merchant, K. A.; Best, R. B.; Louis, J. M.; Gopich, I. V.; Eaton, W. A. *Proc. Natl. Acad. Sci. U.S.A.* **2007**, *104*, 1528−1533.
(17) Samuel, D.; Kumar, T. K. S.; Srimathi, T.; Hsieh, H.; Yu, C. *J. Biol. Chem.* **2000**, *275*, 34968−34975.
(18) Huang, F.; Lerner, E.; Sato, S.; Amir, D.; Haas, E.; Fersht, A. R. *Biochemistry* **2009**, *48*, 3468−3476.
(19) Lopez-Alonso, J. P.; Bruix, M.; Font, J.; Ribo, M.; Vilanova, M.; Jimenez, M. A.; Santoro, J.; Gonzalez, C.; Laurents, D. V. *J. Am. Chem. Soc.* **2010**, *132*, 1621−1630.
(20) Reed, M. A. C.; Jelinska, C.; Syson, K.; Cliff, M. J.; Splevins, A.; Alizadeh, T.; Hounslow, A. M.; Staniforth, R. A.; Clarke, A. R.; Craven, C. J.; Waltho, J. P. *J. Mol. Biol.* **2006**, *357*, 365−372.
(21) Eaton, W. A.; Munoz, V.; Hagen, S. J.; Jas, G. S.; Lapidus, L. J.; Henry, E. R.; Hofrichter, J. *Annu. Rev. Biophys. Biomol. Struct.* **2000**, *29*, 327−359.
(22) Mason, P. E.; Neilson, G. W.; Enderby, J. E.; Saboungi, M. L.; Dempsey, C. E.; MacKerell, A. D.; Brady, J. W. *J. Am. Chem. Soc.* **2004**, *126*, 11462−11470.
(23) Arakawa, T.; Timasheff, S. N. *Biochemistry* **1984**, *23*, 5924−5929.
(24) Courtenay, E. S.; Capp, M. W.; Record, M. T. *Protein Sci.* **2001**, *10*, 2485−2497.
(25) Mason, P. E.; Brady, J. W.; Neilson, G. W.; Dempsey, C. E. *Biophys. J.* **2007**, *93*, L4−L6.
(26) Mehrnejad, F.; Khadem-Maaref, M.; Ghahremanpour, M. M.; Doustdar, F. *J. Comput.-Aided Mol. Des.* **2010**, *24*, 829−841.
(27) Hunger, J.; Niedermayer, S.; Buchner, R.; Hefter, G. *J. Phys. Chem. B* **2010**, *114*, 13617−13627.
(28) O'Brien, E. P.; Dima, R. I.; Brooks, B.; Thirumalai, D. *J. Am. Chem. Soc.* **2007**, *129*, 7346−7353.
(29) England, J. L.; Haran, G. *Annu. Rev. Phys. Chem.* **2011**, *62*, 257−277.
(30) Lim, W. K.; Rosgen, J.; Englander, S. W. *Proc. Natl. Acad. Sci. U.S.A.* **2009**, *106*, 2595−2600.
(31) Mountain, R. D.; Thirumalai, D. *J. Phys. Chem. B* **2004**, *108*, 19711−19716.
(32) Batchelor, J. D.; Olteanu, A.; Tripathy, A.; Pielak, G. J. *J. Am. Chem. Soc.* **2004**, *126*, 1958−1961.
(33) Scott, J. N.; Nucci, N. V.; Vanderkooi, J. M. *J. Phys. Chem. A* **2008**, *112*, 10939−10948.

(34) Mason, P. E.; Neilson, G. W.; Dempsey, C. E.; Barnes, A. C.; Cruickshank, J. M. *Proc. Natl. Acad. Sci. U.S.A.* **2003**, *100*, 4557−4561.
(35) Leberman, R.; Soper, A. K. *Nature* **1995**, *378*, 364−366.
(36) Mason, P. E.; Dempsey, C. E.; Neilson, G. W.; Brady, J. W. *J. Phys. Chem. B* **2005**, *109*, 24185−24196.
(37) Dempsey, C. E.; Mason, P. E.; Bracly, J. W.; Neilson, G. W. *J. Am. Chem. Soc.* **2007**, *129*, 15895−15902.
(38) Gouda, H.; Torigoe, H.; Saito, A.; Sato, M.; Arata, Y.; Shimada, I. *Biochemistry* **1992**, *31*, 9665−9672.
(39) Case, D. A.; Darden, T. A.; Cheatham, T. E. III; Simmerling, C. L.; Wang, J.; Duke, R. E.; Luo, R.; Merz, K. M.; Pearlman, D. A.; Crowley, M.; Walker, R. C.; Zhang, W.; Wang, B.; Hayik, S.; Roitberg, A.; Seabra, G.; Wong, K. F.; Paesani, F.; Wu, X.; Brozell, S.; Tsui, V.; Gohlke, H.; Yang, L.; Tan, C.; Mongan, J.; Hornak, V.; Cui, G.; Beroza, P.; Mathews, D. H.; Schafmeister, C.; Ross, W. S.; Kollman, P. A. *AMBER 9*; University of California: San Francisco, 2006.
(40) Wang, J. M.; Cieplak, P.; Kollman, P. A. *J. Comput. Chem.* **2000**, *21*, 1049−1074.
(41) Berendsen, H. J. C.; Grigera, J. R.; Straatsma, T. P. *J. Phys. Chem.* **1987**, *91*, 6269−6271.
(42) Jorgensen, W. L.; Tiradorives, J. *J. Am. Chem. Soc.* **1988**, *110*, 1657−1666.
(43) MacKerell, A. D.; Bashford, D.; Bellott, M.; Dunbrack, R. L.; Evanseck, J. D.; Field, M. J.; Fischer, S.; Gao, J.; Guo, H.; Ha, S.; Joseph-McCarthy, D.; Kuchnir, L.; Kuczera, K.; Lau, F. T. K.; Mattos, C.; Michnick, S.; Ngo, T.; Nguyen, D. T.; Prodhom, B.; Reiher, W. E.; Roux, B.; Schlenkrich, M.; Smith, J. C.; Stote, R.; Straub, J.; Watanabe, M.; Wiorkiewicz-Kuczera, J.; Yin, D.; Karplus, M. *J. Phys. Chem. B* **1998**, *102*, 3586−3616.
(44) Jorgensen, W. L.; Chandrasekhar, J.; Madura, J. D.; Impey, R. W.; Klein, M. L. *J. Chem. Phys.* **1983**, *79*, 926−935.
(45) Ryckaert, J. P.; Ciccotti, G.; Berendsen, H. J. C. *J. Comput. Phys.* **1977**, *23*, 327−341.
(46) Darden, T.; York, D.; Pedersen, L. *J. Chem. Phys.* **1993**, *98*, 10089−10092.
(47) Bai, Y. W.; Karimi, A.; Dyson, H. J.; Wright, P. E. *Protein Sci.* **1997**, *6*, 1449−1457.
(48) Bottomley, S. P.; Popplewell, A. G.; Scawen, M.; Wan, T.; Sutton, B. J.; Gore, M. G. *Protein Eng.* **1994**, *7*, 1463−1470.
(49) Vu, D. M.; Peterson, E. S.; Dyer, R. B. *J. Am. Chem. Soc.* **2004**, *126*, 6546−6547.
(50) Gao, Y. Q. *J. Chem. Phys.* **2008**, *128*, 064105/1−064105/5.
(51) Shao, Q.; Gao, Y. Q. *J. Chem. Phys.* **2011**, *135*, 135102/1−135102/12.
(52) Tanford, C. *Adv. Protein Chem.* **1968**, *23*, 121−282.
(53) Tanford, C. *Adv. Protein Chem.* **1970**, *24*, 1−95.
(54) Scholtz, J. M.; Barrick, D.; York, E. J.; Stewart, J. M.; Baldwin, R. L. *Proc. Natl. Acad. Sci. U.S.A.* **1995**, *92*, 185−189.
(55) Street, T. O.; Bolen, D. W.; Rose, G. D. *Proc. Natl. Acad. Sci. U.S.A.* **2006**, *103*, 13997−14002.
(56) Auton, M.; Bolen, D. W.; Rosgen, J. *Proteins* **2008**, *73*, 802−813.
(57) Timasheff, S. N. *Adv. Protein Chem.* **1993**, *22*, 67−97.
(58) Timasheff, S. N. *Proc. Natl. Acad. Sci. U.S.A.* **2002**, *99*, 9721−9726.
(59) Hong, J.; Capp, M. W.; Anderson, C. E.; Record, M. T. *Biophys. Chem* **2003**, *105*, 517−532.
(60) Pegram, L. M.; Record, M. T., Jr. *Methods Mol. Biol.* **2009**, *490*, 179−193.
(61) Baynes, B. M.; Trout, B. L. *J. Phys. Chem. B* **2003**, *107*, 14058−14067.
(62) Kang, M.; Smith, P. E. *Fluid Phase Equilib.* **2007**, *256*, 14−19.
(63) Smith, P. E. *Biophys. J.* **2006**, *91*, 849−856.
(64) Shimizu, S.; Boon, C. L. *J. Chem. Phys.* **2004**, *121*, 9147−9155.
(65) Shimizu, S. *Chem. Phys. Lett.* **2011**, *514*, 156−158.
(66) Lee, M. E.; van der Vegt, N. F. A. *J. Am. Chem. Soc.* **2006**, *128*, 4948−4949.
(67) Ganguly, P.; Mukherj, D.; Junghans, C.; van der Vegt, N. F. A. *J. Chem. Theory Comput.* **2012**, *8*, 1802−1807.
(68) Graziano, G. *Phys. Chem. Chem. Phys.* **2011**, *13*, 17689−17695.
(69) Graziano, G. *Phys. Chem. Chem. Phys.* **2011**, *13*, 12008−12014.
(70) Godawat, R.; Jamadagni, S. N.; Garde, S. *J. Phys. Chem. B* **2010**, *114*, 2246−2254.
(71) Collins, K. D. *Biophys. J.* **1997**, *72*, 65−76.
(72) Collins, K. D. *Methods* **2004**, *34*, 300−311.
(73) Wei, H.; Fan, Y.; Gao, Y. Q. *J. Phys. Chem. B* **2010**, *114*, 557−568.
(74) Wei, H.; Shao, Q.; Gao, Y. Q. *Phys. Chem. Chem. Phys.* **2010**, *12*, 9292−9299.
(75) Wei, H.; Yang, L.; Gao, Y. Q. *J. Phys. Chem. B* **2010**, *114*, 11820−11826.
(76) Tobi, D.; Elber, R.; Thirumalai, D. *Biopolymers* **2003**, *68*, 359−369.